sustainability

MDPI

Article

Year-Round Testing of Coastal Waters of the Gulf of Gdańsk in the Baltic Sea for Detecting Oil in a Seawater Column Using the Fluorescence Method

Emilia Baszanowska * and Zbigniew Otremba

Department of Physics, Gdynia Maritime University, 81-225 Gdynia, Poland; z.otremba@wm.umg.edu.pl
* Correspondence: e.baszanowska@wm.umg.edu.pl; Tel.: +48-58-5586-588

Abstract: Progressive climate changes and the increase in the occurrence of extreme weather phenomena indicate the need to take action to mitigate the negative effects of climate change. One of the main factors affecting climate change is the state of waters that transport heat. Oil pollution present in the water contributes to the absorption of radiation and physico-chemical changes in the sea, which has an impact on the marine ecosystem. This indicates the need to develop methods for effective oil spill detection. This study aimed to improve the methods of early detection of threats related to oil spills in the marine environment, especially when the source of oil may be invisible in the depths of the sea. Therefore, the method based on the fluorometric index is proposed, and its effectiveness for oil detection in seawater is studied. The study has answered the question of how biological activity during a whole year influences the effectiveness of oil detection by the proposed fluorometric index method. Therefore, for the calculation of the fluorometric index, the changes in the seawater fluorescence spectrum in the ultraviolet range were determined, which occurred under the influence of diffusion of some oil components in the sea. The principle of detection of oil contaminants based on the excitation-emission fluorescence spectrum is described. For the measurements, natural seawater samples used in the laboratory were exposed to a mixture of crude oil and oils commonly found in navigation. The effectiveness of oil substance detection using the fluorometric index in the biologically productive and unproductive seasons was analyzed for seawater in the vicinity of Gdynia and Gdansk ports in Poland in northern Europe. The results of excitation-emission spectra and fluorometric index indicate that the changes in the biological activity during the year do not affect the detectability of oil present in seawater for the considered oil-to-water ratio. Summarize the sensitivity analysis of the method indicates the possibility of detection of oil contamination regardless of the season. The obtained results pave the way for the construction of an underwater device to detect oil in the vicinity of such a detector.

Keywords: oil detection; seawater; excitation-emission spectra (EEMs); fluorometric index; water column

check for updates

Citation: Baszanowska, E.; Otremba, Z. Year-Round Testing of Coastal Waters of the Gulf of Gdańsk in the Baltic Sea for Detecting Oil in a Seawater Column Using the Fluorescence Method. *Sustainability* **2023**, *15*, 9898. https://doi.org/10.3390/su15139898

Academic Editors: Ee Von Lau and Guozhong Wu

Received: 29 April 2023
Revised: 8 June 2023
Accepted: 19 June 2023
Published: 21 June 2023

Copyright: © 2023 by the authors. Licensee MDPI, Basel, Switzerland. This article is an open access article distributed under the terms and conditions of the Creative Commons Attribution (CC BY) license (https://creativecommons.org/licenses/by/4.0/).

1. Introduction

Spills of crude oil and its derivatives into the marine environment result mainly from human activity and constitute a significant ecological threat. The cause of the leakage of petroleum substances into the seas and oceans is the consequence of sea transport, sinking of tankers or shipwrecks on the seabed, as well as damage to pipelines or drilling platforms [1–4]. The last largest oil spill into the ocean waters took place in 2010 on the "Deepwater Horizon" drilling rig in the Gulf of Mexico. This catastrophe contributed to the extinction of some species of flora and a huge disruption of the marine ecosystem [5–7]. A possible source of oil pollution in a marine environment may also be the leakage of ship consumables. Some sources of oil pollution can be underwater, e.g., oil spills, spills from pipelines, shipwrecks, and even natural seepage of oil from the seabed. Oil contaminants generated underwater may not show up on the sea surface or may become visible with considerable delay far from where they originate.

It is likely that crude oil and its processing products will play a lesser role as a source of energy in the global economy in the future. This is primarily about decreasing carbon dioxide emissions. However, oil production is not currently decreasing, and its sea transport in the years 2010–2018 increased from 1867 to 2030 million cubic meters. Only the years 2020 and 2021 were marked by a decrease in the volume of transported crude oil to the level of 2010 (due to the pandemic) [8]. It can be assumed that tankers transporting crude oil will continue to travel sea routes for several decades to come. For many years, research has been conducted on the harmfulness of hydrocarbon substances for specific organisms as well as for the entire marine ecosystem. The entry of crude oil and hydrocarbon products into the marine environment cannot be prevented [9].

One of the sustainable development goals is to protect the oceans, seas and marine resources and to use them in a sustainable manner. As part of this objective, the prevention, reduction and elimination of marine pollution is an important task. Therefore, for the care of the environment, various legal regulations have been introduced [10], as well as regional and national legal arrangements aimed at eliminating oil pollution in the marine environment [11]. Illegal oil discharges are much less numerous now than they were a few decades ago, but it is still impossible to stop them [12]. Achieving this task in relation to oil pollution in the marine environment will be possible with the development of methods for early detecting oil pollution and determining its source. Therefore, to protect the marine environment, it is important to develop technologies and methods of oil detection to improve the accuracy, sensitivity and efficiency of detecting oil in seawater and responding to oil spill incidents. There are many different oil detection methods that are used both offshore and remotely [13–15]. The detection of oil in water depends on many factors: the type of oil, its form, i.e., an oil film on the water surface, a form dissolved in the seawater column, or an oil emulsion. In addition, the detection of oil in water is also affected by atmospheric conditions. Therefore, various methods are used to detect oil in water [15,16]. However, to quickly and effectively detect oil in water, models are being developed based on a combination of different technologies, including remote satellite observations, spectral analysis, chemical detectors and monitoring systems. This makes it possible to quickly and effectively detect oil spills at sea, which allows for a quick response and minimization of negative effects on the marine environment. However, these models require input data that is obtained from marine monitoring studies. The data from this article can be used as input data for operational models to track marine components.

As it was mentioned above, oil detection in seawater depends, among others, on the type of oils. Most liquid hydrocarbon substances have a density lower than water, and reveal on the sea as an oil film. Light oil fractions undergo a rapid evaporation process and are released into the air, while heavy ones settle to the bottom. The oil palm moves with the wind and, under the influence of the waves, is dissolved and emulsified and penetrates the deeper layers of water. Detection of surface pollutants at sea is possible. The simplest method is aerial surveillance (human vision, cameras, ultraviolet and infrared scanners, and measurement of thermal radiation) [13,17,18]. Unfortunately, the optical remote sensing method has limitations due to atmospheric conditions and the availability of daylight. However, the optical method has a unique spectral analysis which can distinguish oil spills [18,19]. Passive remote sensing methods used in the ultraviolet range, visible range or near-infrared are used for oil detection end estimation of the oil plum thickness [20]. Recently, radar technology (Synthetic Aperture Radar—SAR) has become the dominant technique [21,22]. Due to the lack of restrictions related to weather conditions and access to daylight, active microwave sensors are commonly used [23]. Within Europe, maritime safety activities are handled by the European Maritime Safety Agency—EMSA [24]. The CleanSeaNet system operates within this institution [25], under which images of the sea surface indicating places potentially contaminated with oil are distributed.

Crude oil and most liquid products of its refinery processing contain substances that penetrate into the water and diffuse in it. Detection of oil under the sea surface is much more difficult, and in that case, remote sensing methods such as advanced laser fluorometry

(ALF), laser-induced fluorescence (LIF) or UV-induced fluorescence [26–29] and various in situ methods [30–32] are used. Moreover, various types of underwater sensors based on the ability to detect the fluorescence of excited oil components in the UV range [14,33–35] are also used. Natural seawater constituents exhibit optical properties [36,37] such as absorption [38–40], fluorescence in excitation-emission (EEM) spectra [41–46], and other similarities to oil substances. However, the possibility of detecting oily substances in water by analyzing the fluorescence spectra has been confirmed [47]. This is achieved by the fluorescence index, which is a measure of the EEM transformation of seawater as a result of contamination with oil substances.

Taking into account the current state of knowledge, oil detection under the sea surface for individual layers of water in the water column should be developed to improve the efficiency of oil detection. Therefore, the authors have developed optical methods for detecting oil that has leaked into the sea. It is expected that the results of such tests will be helpful in the design of devices that signal the appearance of a leak of oil substances, whether on the surface of the water or in the depths.

The objective of the study involved examining the Fluorometric index FI to oil detection in relation to the biological activity in the seawater on the Polish coast of the Baltic Sea in northern Europe for individual months, productive and unproductive seasons of the year. The obtained data will indicate if biological activity disturbed the oil detection in seawater in the considered oil-to-water ratio ($r_{o/w}$).

The aim of the activities described in this paper is to indicate the effectiveness of oil detection in a possible oil spill in the coastal areas of the sea based on the proposed fluorometric index FI. The criteria for the check of the correct operation of the FI (in order to know whether the sea water is oil polluted or unpolluted) have been precisely defined. FI values above 1 inform about the presence of oil in water, while FI values below 1 indicate that the seawater is free of oil. It allows for signaling the presence of oil in seawater. The specified criteria for FI allow it to be used in the future with a fluorometric device located in the vicinity of a potential oil spill hazard or in a place subject to special protection. The study analyzed the modification of seawater fluorescence spectra and the fluorescence indicator for oil detection under the influence of oil substances, which occurs in particular months throughout the year. The effectiveness of FI is studied in relation to biological activity changes during a particular month throughout the whole year for an oil-in-water ratio range of 0.5–500 $\times$ 10^{-6}. The obtained results indicated that in the considered oil-to-water ratio range, the changes in biological activity do not disturb the detection of oil present in seawater.

2. Materials and Methods

2.1. Studied Area

The current study examined the effect of oil pollution on the fluorescence spectrum of seawater samples collected monthly from April 2019 to March 2020 from coastal waters of the Gulf of Gdańsk in Poland in northern Europe.

2.2. Seawater Samples

The sampling point was located at the end of the walking pier in Gdynia-Orłowo (Figure 1). Seawater samples were collected for particular months during the whole year in the water column from a depth of 1 m into one-liter glass bottles. Seawater samples were collected using a water scoop with a 1 L glass cylinder with a measure set at a depth of 1 m. Each month, seawater was collected simultaneously into two one-liter bottles.

Natural seawater is characterized by the biological activity of natural sweater constituents. In the Gulf of Gdansk of the Baltic Sea in Poland, productive and unproductive seasons are distinguished during the whole year. The biological activity for the productive and unproductive seasons was presented in Table 1 by the physical and biological parameters of natural seawater samples [48]. During the productive season (spring, summer, and early autumn, from April to October), phytoplankton production was substantially

increased. Conversely, during the unproductive season (late autumn, winter, and early spring, from November to March), the level of biological activity was low, which is reflected in the low phytoplankton production.

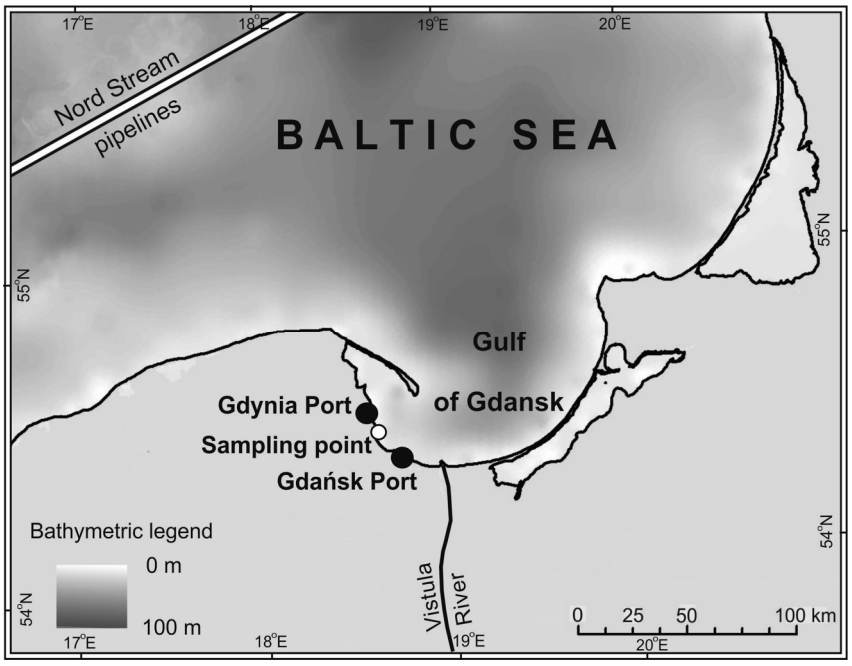


Figure 1. Location of the seawater sampling point in Gdynia Orłowo in the Gulf of Gdańsk in Poland in northern Europe (54°28′46″ N 18°33′59″).

Table 1. The physical and biological parameters of natural seawater samples, for particular months within one year from April 2019 to March 2020, sampled from the coastal waters of the Gulf of Gdansk [48].

	April	May	June	July	August	September	October	November	December	January	February	March
Temperature [°C]	4.97	8.44	14.6	20.4	17.8	17.4	14.3	8.75	7.58	5.25	4.5	4.69
Primary production [mg m^{-2} d^{-1}]	21.7	40	27.4	2.35	8.32	5.3	80.6	0.24	0.08	0.03	0.71	44.1
Phytoplankton [mg m^{-3}]	75.3	105	77.4	20.2	30.8	46.4	122	9.1	2.1	0.4	1.6	96.6

2.3. Oil Contaminant

As shown in Figure 2, sources of seawater contamination by oil substances can vary. As a consequence of this, a variety of types of petroleum substances can appear in the sea. A mixture of crude oils, fuels, and lubricating oils as a polluting medium was applied to the measurements. The oil mixture was prepared in a way to ensure that each kind of oil made an equal contribution to the overall volume. Next, to achieve an appropriate oil-to-water ratio ($r_{o/w}$), the mixture of oils was weighed out on the aluminum foil and used for contamination of oil-free seawater in the oil-to-water ratio ($r_{o/w}$) range of 500–0.5 × 10^{-6}. The individual components of the oil blend exhibit similar fluorescence when in contact with water.

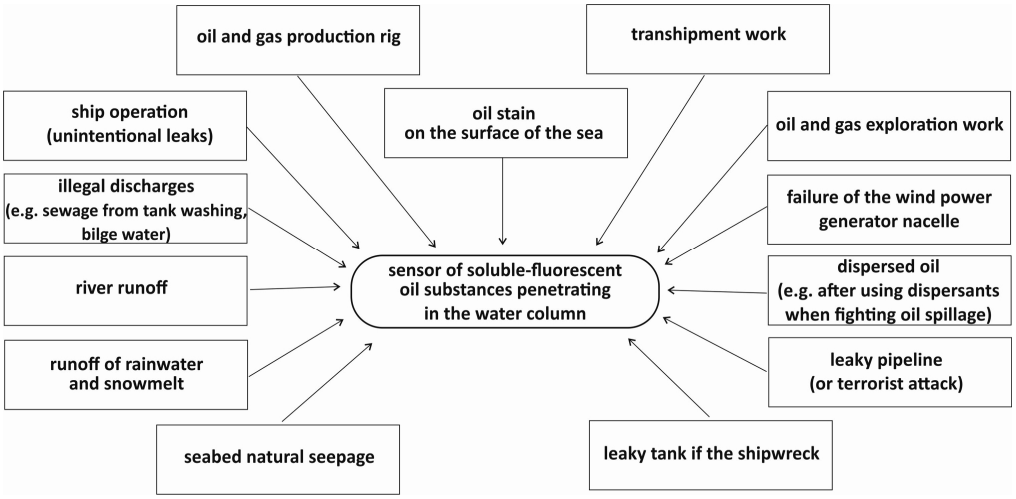


Figure 2. Possible origin of oil trace.

2.4. Apparatus and Data Processing

For the measurements of the full excitation-emission spectrum (EEMs), a Hitachi F-7000 FL spectrofluorometer was used with the monochromator for the selection of wavelengths and a Xenon Flash Lamp as the source of excited light. For the determination of EEM spectra a 1 cm by 1 cm quartz cuvette was used. The instrument settings used were as follows: the excitation wavelength was 200–400 nm, the emission wavelength was 260–600 nm with a 5 nm step for the width of the slit for the excitation and emission wavelength of 10 nm, with the photomultiplier voltage set to 400 V and the time of integration set to 0.5 s. Microsoft Excel 2019 SNGL OLP NL Acdmc was used to process the data of the determined excitation-emission spectra (EEMs).

3. Results and Discussion

Monthly water sampling made it possible to determine the scale of the impact of changes in the optical properties of seawater on the ability to detect oil throughout the whole year. The phenomenon of seawater fluorescence manifests itself in the ultraviolet range in the form of peaks derived from the fluorescence of several characteristic types of chemical compounds in the literature described by the wavelength-independent fluorescence maximum $\lambda_{Ex}/\lambda_{Em}$ in the EEM spectrum. $\lambda_{Ex}/\lambda_{Em}$ describes the maximum fluorescence for excitation wavelength related to the emission wavelength [49–53]. The wavelength-independent fluorescence maximum $\lambda_{Ex}/\lambda_{Em}$ based on EEM spectra of natural seawater was determined for all seawater samples in a particular month throughout the whole year. The example EEM spectra of seawater samples taken in April (a) and December (b) as representatives of productive and unproductive seasons in the Baltic Sea are presented in Figure 3. The EMM spectra were determined for $\lambda_{Ex}/\lambda_{Em}$ = 225/355–380, 265/420, 280/380 and 320/415, corresponding to the natural seawater components described in Tables 2 and 3. In the EEM spectra, the differences in natural seawater biological activity over the whole year in the productive and unproductive seasons in the Baltic Sea (Table 1) are reflected through changes in the position of the emission wavelength of the main detected wavelength-independent fluorescence maximum $\lambda_{Ex}/\lambda_{Em}$ = 225/355–380, which corresponds to the tryptophan-like seawater component (T). Specifically, the position of the wavelength-independent fluorescence maximum for the T component is red-shifted to longer emission wavelengths during the unproductive season and blue-shifted to lower emission wavelengths during the productive season (Table 2). The shift of the tryptophan peak towards longer waves during the non-productive period in the Baltic Sea indicates a decrease in biological activity, such as primary production, which is responsible for CDOM biological activity [54]. Furthermore, throughout the year (from April 2019 to March 2020), changes in biological activity were reflected in the determined seawater EEM spectra for

each month by changes in the fluorescence intensity of the main $\lambda_{Ex}/\lambda_{Em}$ = 225/355–380 (T) and other detected $\lambda_{Ex}/\lambda_{Em}$ linked to components of colored dissolved organic matter (CDOM) [49–53] are presented in Table 3. The fluorescence intensity achieved higher values during the productive season (from April to October) than in the unproductive season (from November to March). The increase in the fluorescence intensity values in the productive season is caused by an increase in biological activity, such as primary production. Moreover, it influences the activity of CDOM.

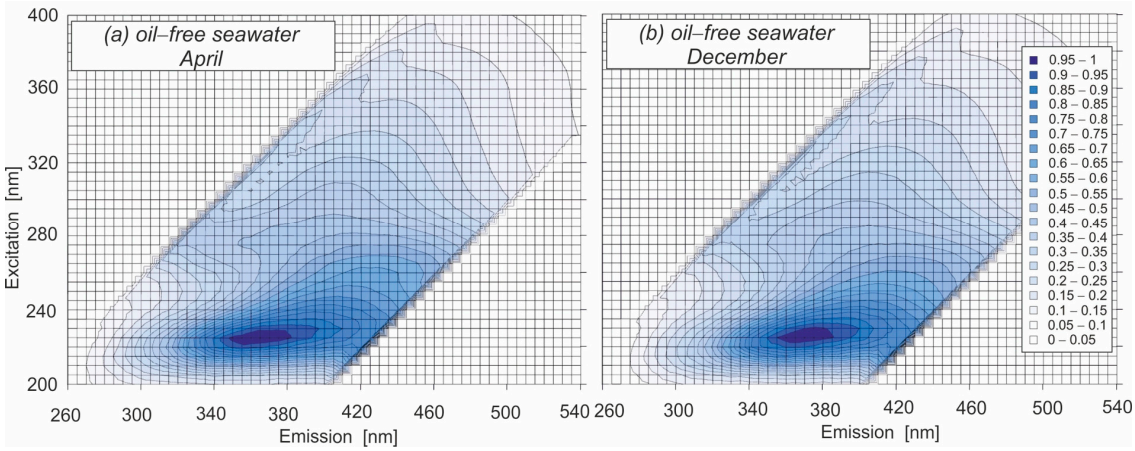


Figure 3. Example EEM spectra for free-of-oil seawater samples.

Table 2. The wavelength-independent fluorescence maximum ($\lambda_{Ex}/\lambda_{Em}$) detected for tryptophan-like T components of seawater from April to December 2019 and from January to March 2020 in the productive and unproductive seasons in the Baltic Sea.

Month	λ_{Ex} [nm]/λ_{Em} [nm]
	(T)
IV	225/360
V	225/365
VI	225/355
VII	225/355
VIII	225/365
IX	225/360
X	225/365
XI	225/370
XII	225/370
I	225/365
II	225/380
III	225/365

Table 3. Changes in the fluorescence intensity in the productive and unproductive part of year in the Baltic Sea from April to December 2019 and from January to March 2020 for the detected wavelength-independent fluorescence maximum $\lambda_{Ex}/\lambda_{Em}$ linked to the seawater components (T)—tryptophan-like component, (A)—humic-like A component, (M)—marine humic-like component, (C) humic-like component C.

Month	Fluorescence Intensity [a.u.]			
$\lambda_{Ex}/\lambda_{Em}$	T 225/355–380	A 265/420	M 280/380	C 320/415
IV	73.21	45.05	30.08	22.82
V	65.68	39.56	26.95	18.82
VI	66.68	37.77	27.66	18.70
VII	71.52	39.04	29.58	18.78
VIII	66.30	38.51	28.90	19.25
IX	61.47	33.94	24.50	17.09
X	62.53	34.04	25.50	17.02
XI	57.75	34.62	23.36	17.46
XII	58.04	32.20	23.27	16.24
I	65.61	38.67	27.01	20.02
II	61.20	37.58	25.59	18.51
III	62.74	37.49	26.11	18.51

Figure 4a,b confirms the influence of changes in biological activity on the fluorescence intensity (Figure 4a) and the position of the emission wavelength of the $\lambda_{Ex}/\lambda_{Em}$ of tryptophan-like seawater component T for the excitation wavelength λ_{ex} = 225 nm (Figure 4b) for the particular months throughout the year. The changes in seawater fluorescence intensity of the tryptophan-like component of seawater for the excitation wavelength λ_{ex} = 225 nm during the productive season (from April to October) and the unproductive season (from November to March) are presented in Figure 4a. The fluorescence intensity of the tryptophan-like seawater component (T) achieves higher values in the productive season than in the unproductive season, which is reflected in Figure 4a. As mentioned above, this is a consequence of the growth of biological activity primary production and CDOM [54]. For the studied case, it is confirmed by the changes in the natural seawater constituents described in Table 1. Figure 4b presents the changes in the position of the emission wavelength of tryptophan-like seawater component T for the excitation wavelength λ_{ex} = 225 nm during the productive season (from April to October) and the unproductive season (from November to March). Shifts in the position of the emission wavelength of the tryptophan-like seawater component to longer emission wavelengths are visible in the unproductive season.

The accuracy of oil determination in seawater can be affected by natural biological activity, which can result in overlapping fluorescence signals between natural seawater components and oil [47]. To address this issue, this study examined the impact of biological activity on oil fluorescence in seawater as reflected in the EEM spectra over the course of a year. The current study analyzed the use of a mixture of oils to contaminate seawater for $r_{o/w}$ ratios in the range of 0.5–500 $\times$ 10^{-6}. In Figure 5A,B, the EEM spectra of seawater contaminated by the mixture of oils for two selected months, April (A) and December (B), with varying levels of biological activity throughout the year ($r_{o/w}$ = 0.5 $\times$ 10^{-6}, 5 $\times$ 10^{-6}, 50 $\times$ 10^{-6}, and 500 $\times$ 10^{-6}) were presented. The EEM spectra of seawater contaminated with the oil mixture in the range of $r_{o/w}$ used in this study were significantly different from those of natural seawater. This analysis aimed to investigate the influence of oil present in seawater on changes in EEMs.

Based on the EEM spectra determined for April (Figure 5A), it can be observed that even for the lowest $r_{o/w}$ (0.5 $\times$ 10^{-6}), there is a clear difference in the EEM spectrum shape compared to natural seawater. It is caused by the high similarity of natural seawater with oil-polluted seawater in the case of the lowest $r_{o/w}$ (0.5 $\times$ 10^{-6}). It means that oil is not dominant in the sample. For that level of $r_{o/w}$ (0.5 $\times$ 10^{-6}), the presence of natural seawater constituents is manifested by changes in the EEMs. The EEM spectra of seawater polluted by the mixture of oil exhibited excitation-emission peaks ($\lambda_{Ex}/\lambda_{Em}$) that changed with the $r_{o/w}$. Even for the lowest $r_{o/w}$, the EEMs peaks 225/340 and 265/325 caused by the oil presence in seawater were detected. The EEM peaks changed with a 10, 100, and 1000 times increase in $r_{o/w}$. For 100 times increased $r_{o/w}$, the peak $\lambda_{Ex}/\lambda_{Em}$ = 215/290 was detected, while for 1000 times increased $r_{o/w}$, a new peak $\lambda_{Ex}/\lambda_{Em}$ = 290/265 was detected. Furthermore, as the $r_{o/w}$ increased, the position of the main peak 1 shifted to lower excitation and emission wavelengths λ_{Ex} = 220 nm and λ_{Em} = 335 nm, respectively. Similar peaks were observed for December (Figure 5B) when the biological activity was low. Only minor changes in the detected EEM peaks were found for lower $r_{o/w}$ = 0.5 $\times$ 10^{-6} and 5 $\times$ 10^{-6}. These results suggest that the biological activity does not significantly affect the oil present in seawater for the considered $r_{o/w}$ range from 50 to 500 $\times$ 10^{-6}. To confirm the independence of the EEMs peaks from the biological activity throughout the year, the EEMs peaks were determined for each month from April 2019 to March 2020 for all considered $r_{o/w}$. The detected EEM peaks of oily polluted seawater were analyzed in Table 4 for the productive season and Table 5 for the unproductive season in the Baltic Sea. Consistent with the EEM spectra obtained for oil-polluted seawater, similar peaks were detected when the fluorescence of natural seawater was subtracted, as observed in the EEMs presented in Figure 6.

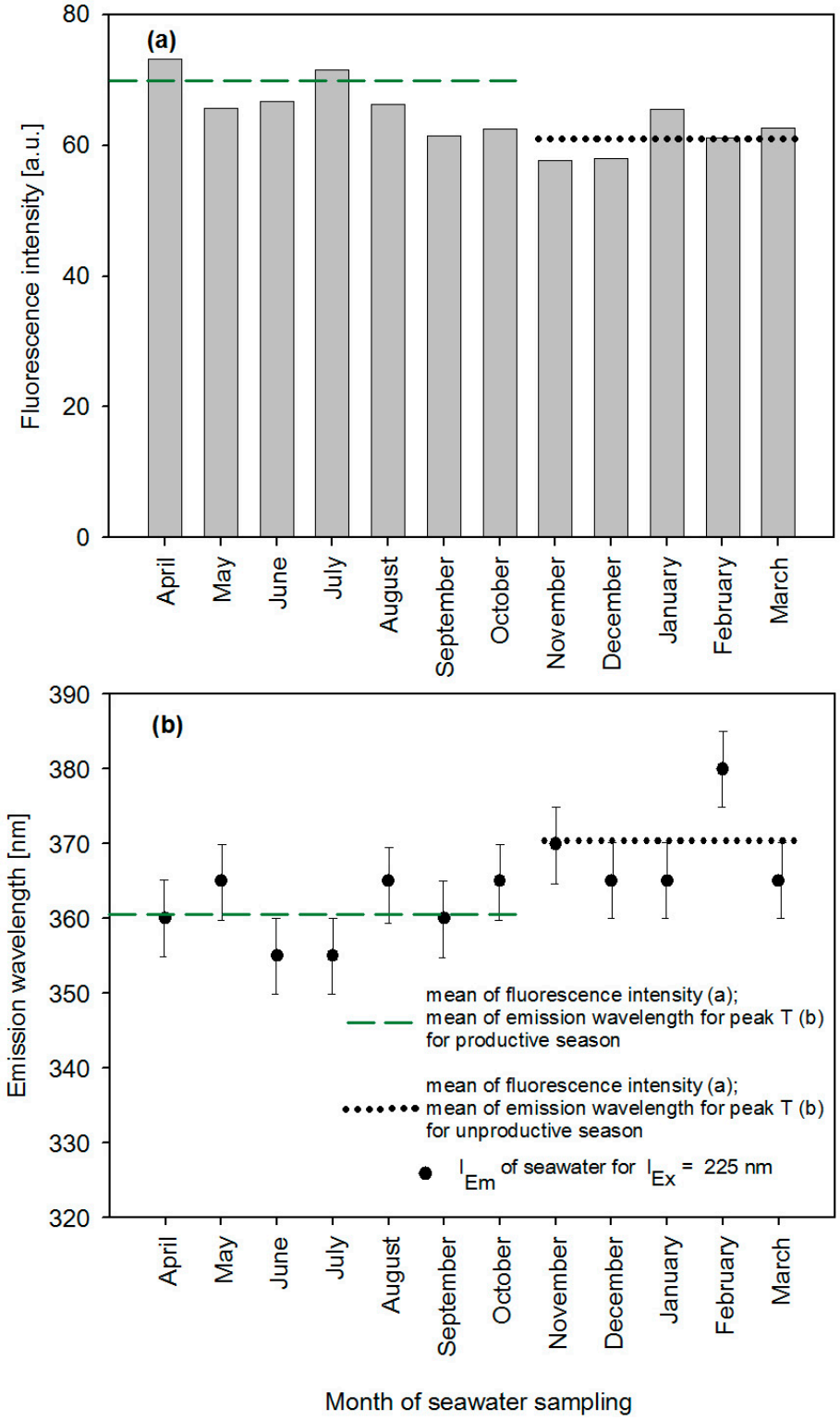


Figure 4. Changes in seawater fluorescence intensity (**a**) and the position for emission wavelength (λ_{Em}) (**b**) of the tryptophan-like component of seawater for the excitation wavelength λ_{Ex} = 225 nm during the year. The broken green line and the line with black dots describe, respectively: the mean of the fluorescence intensity in (**a**) and the mean of the emission wavelength for the position of excitation wavelength 225 nm of the tryptophan-like component T of seawater in (**b**) for the productive season; the mean of the fluorescence intensity in (**a**) and the mean of the emission wavelength for the position of excitation wavelength 225 nm of tryptophan-like component T of seawater in (**b**) during the unproductive season.

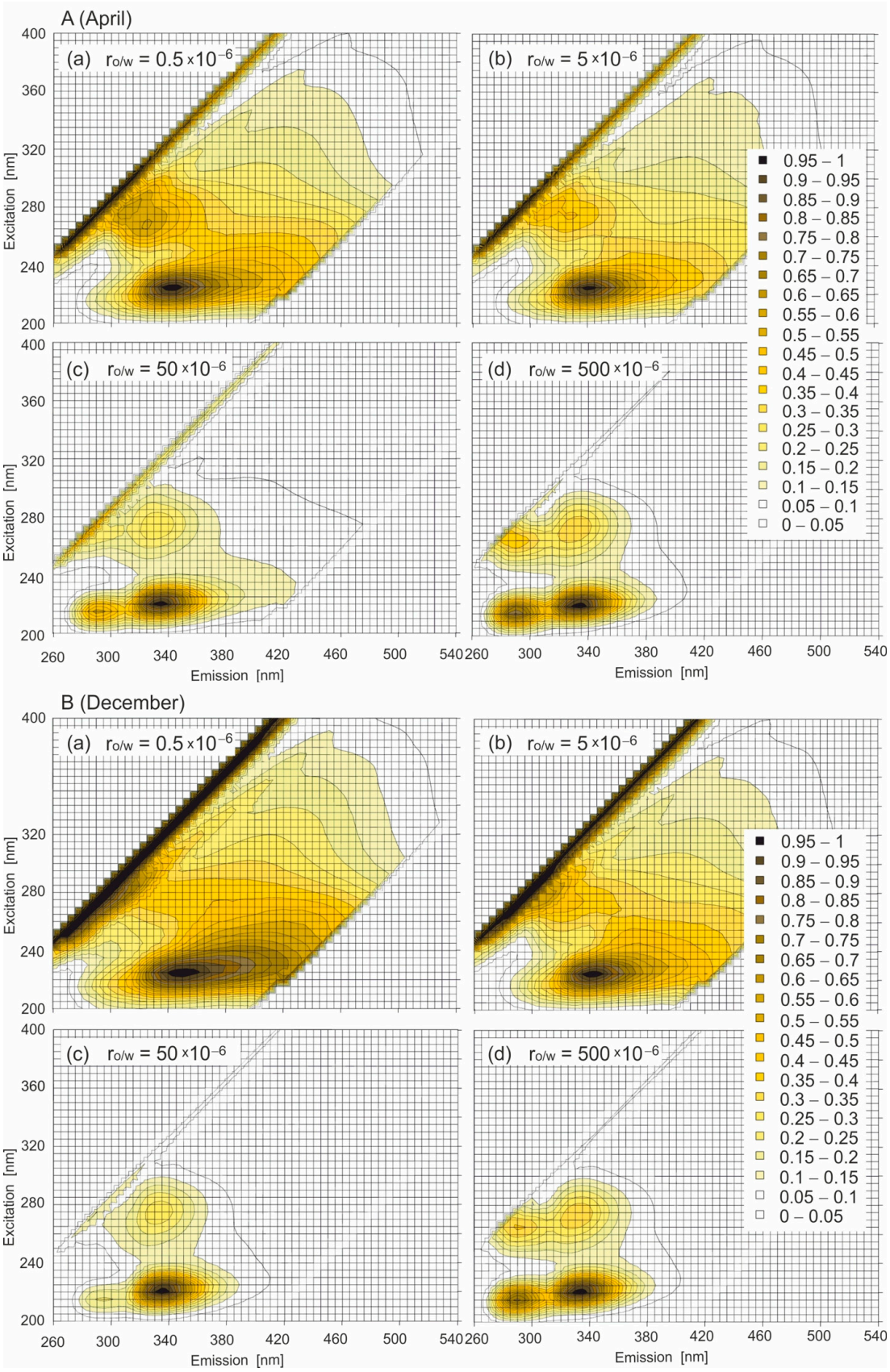


Figure 5. EEMs of seawater polluted with oil as a contour map visualization in 2D for April (**A**) and December (**B**) for various $r_{o/w}$: 0.5×10^{-6} (**a**), 5×10^{-6} (**b**), 50×10^{-6} (**c**) and 500×10^{-6} (**d**) for two selected months from the entire year.

Table 4. Major fluorescent peaks for seawater samples polluted with oil at various oil-to-water ratios ($r_{o/w}$) with their wavelength-independent fluorescence maxima $\lambda_{Ex}/\lambda_{Em}$ for the productive season in the Baltic Sea from April to October 2019.

	λ_{Ex} [nm] ± 5 [nm]/λ_{Em} [nm] ± 5 [nm]				
April	$r_{o/w}$	Peak 1	Peak 2	Peak 3	Peak 4
	0.5×10^{-6}	225/345			265/325
	5×10^{-6}	225/340			270/330
	50×10^{-6}	220/335	215/290		275/335
	500×10^{-6}	220/335	215/290	290/265	275/335
May					
	0.5×10^{-6}	225/345	215/305		275/340
	5×10^{-6}	225/340			275/340
	50×10^{-6}	220/335	215/295		275/330
	500×10^{-6}	220/335	215/290	300/265	275/335
June					
	0.5×10^{-6}	225/355		255/360	275/320
	5×10^{-6}	225/340			275/340
	50×10^{-6}	220/335	215/295		275/335
	500×10^{-6}	220/335	215/290	290/265	275/330
July					
	0.5×10^{-6}	225/345			275/340
	5×10^{-6}	225/340		255/365	275/340
	50×10^{-6}	220/335	215/295		275/335
	500×10^{-6}	220/335	215/290		275/330
August					
	0.5×10^{-6}	225/345			270/340
	5×10^{-6}	225/340			275/335
	50×10^{-6}	220/335	215/290		275/335
	500×10^{-6}	220/335	215/290	295/265	275/330
September					
	0.5×10^{-6}	225/345			270/340
	5×10^{-6}	225/340			275/330
	50×10^{-6}	220/335	215/290		270/330
	500×10^{-6}	220/335	215/290	295/265	275/330
October					
	0.5×10^{-6}	225/340			275/330
	5×10^{-6}	225/340			275/330
	50×10^{-6}	220/335	215/290		275/335
	500×10^{-6}	220/335	215/290	295/265	275/330

Table 5. Major fluorescent peaks for seawater samples polluted with oil at oil-to-water ratios ($r_{o/w}$) with their wavelength-independent fluorescence maxima $\lambda_{Ex}/\lambda_{Em}$ for the unproductive season in the Baltic Sea from November to March 2019–2020.

	λ_{Ex} [nm] ± 5 [nm]/λ_{Em} [nm] ± 5 [nm]				
November	$r_{o/w}$	Peak 1	Peak 2	Peak 3	Peak 4
	0.5×10^{-6}	225/340			280/340
	5×10^{-6}	225/340			275/340
	50×10^{-6}	220/335	215/290		275/330
	500×10^{-6}	220/335	215/290	295/265	275/330

Table 5. *Cont.*

	λ_{Ex} [nm] ± 5 [nm]/λ_{Em} [nm] ± 5 [nm]			
December				
0.5×10^{-6}	225/350			
5×10^{-6}	225/340			270/330
50×10^{-6}	220/335	215/295		275/335
500×10^{-6}	220/335	215/290	295/260	275/330
January				
0.5×10^{-6}	225/355			
5×10^{-6}	225/340			
50×10^{-6}	220/335	215/295		275/335
500×10^{-6}	220/340	215/295	290/265	275/330
February				
0.5×10^{-6}	225/355			
5×10^{-6}	225/350			275/335
50×10^{-6}	220/335	220/295		275/335
500×10^{-6}	220/335	215/290	290/265	275/330
March				
0.5×10^{-6}	225/345			
5×10^{-6}	225/340			275/330
50×10^{-6}	220/335	215/295		275/330
500×10^{-6}	220/335	215/290	290/265	275/330

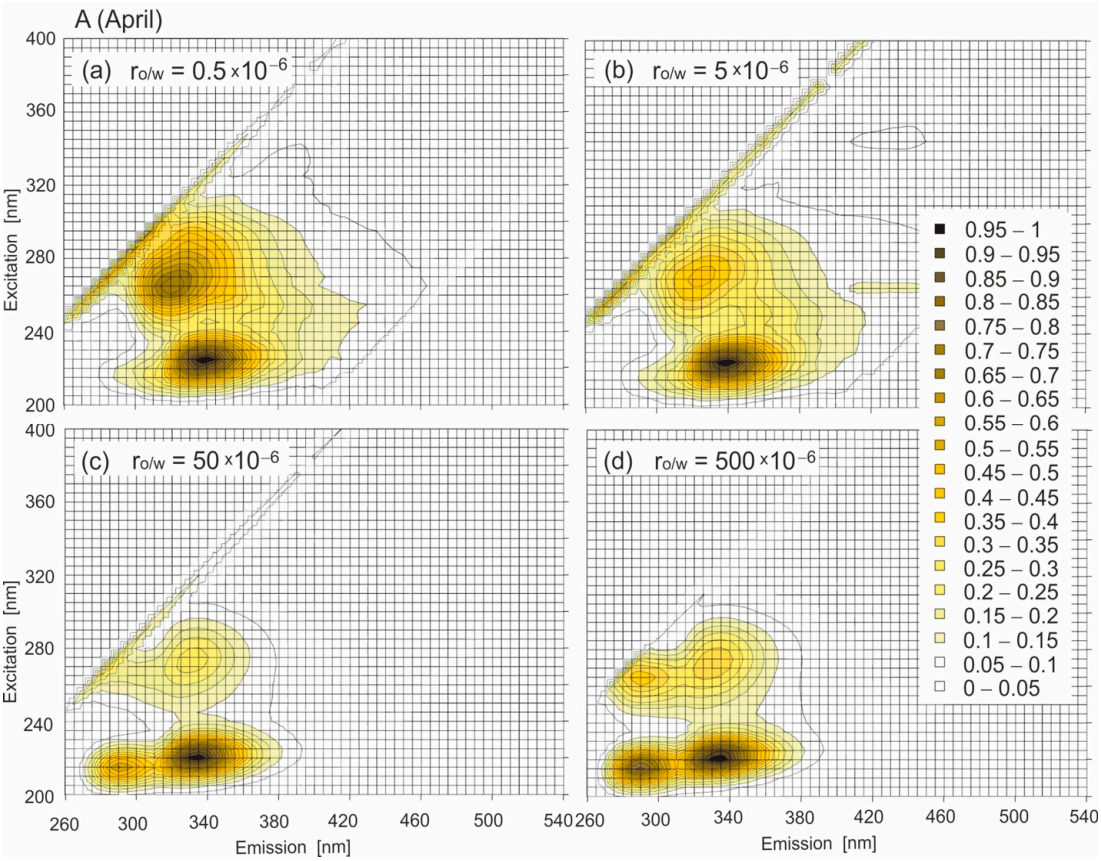


Figure 6. *Cont.*

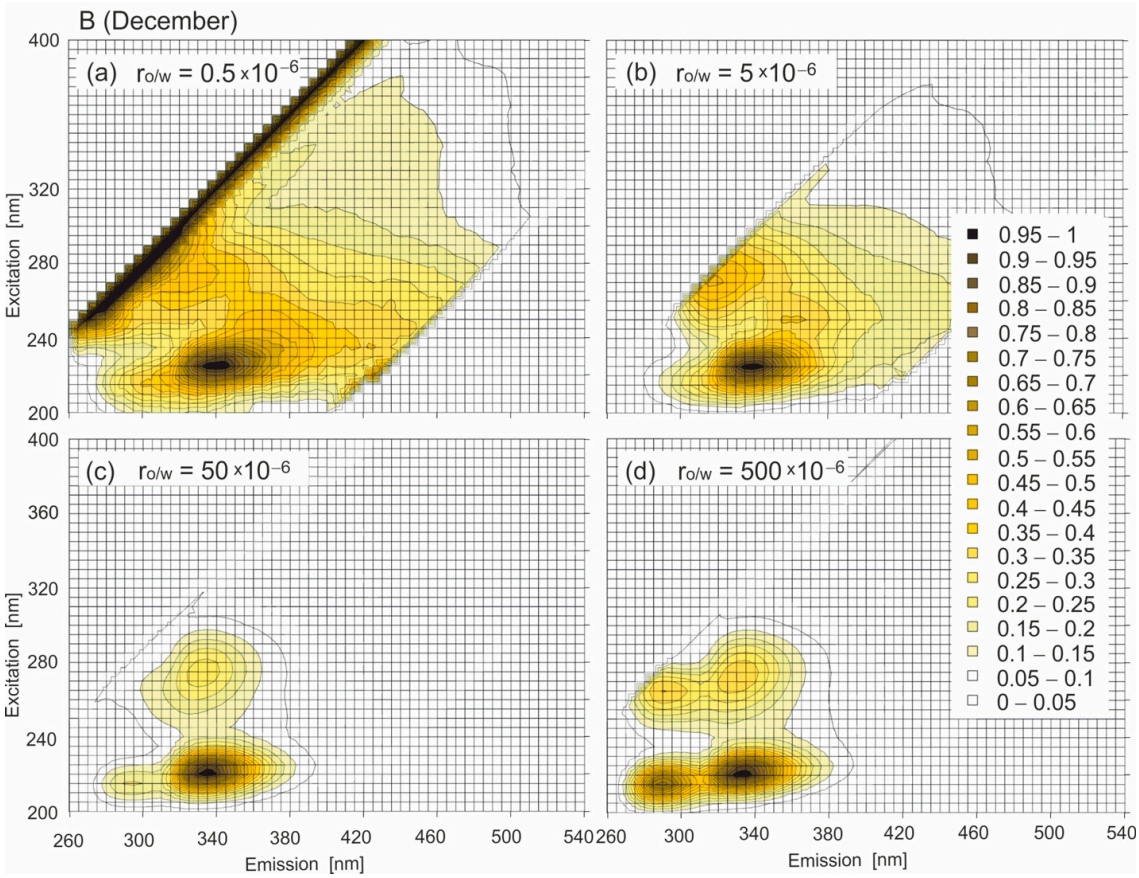


Figure 6. EEMs of oil-polluted seawater for April (**A**) and December (**B**) in the case when the fluorescence of oil-free seawater was subtracted for various $r_{o/w}$.

The analysis of the determined $\lambda_{Ex}/\lambda_{Em}$ for particular $r_{o/w}$ indicates that for the highest $r_{o/w}$ in EEMs are detected four different $\lambda_{Ex}/\lambda_{Em}$, while for the lowest $r_{o/w,}$ only two $\lambda_{Ex}/\lambda_{Em}$ were determined. The interpretation of the results indicates that higher values of oil indicate that oil substances are dominant in the seawater and are responsible for the fluorescence.

It can be concluded that EEM measurement is an effective method for detecting oil in seawater within the $r_{o/w}$ range of 0.5–500 $\times$ 10^{-6}. However, EEM measurements can be time-consuming. To address this, a fluorometric index (FI) was used as a parameter to oil presence in water. Parameter FI was defined as a quotient of the fluorescence intensity of oil-polluted seawater at the emission wavelength to the fluorescence intensity of oil-free seawater at the same maximum excitation wavelength for both polluted and oil-free seawater (Equation (1)) [51–53]. The FI can be calculated using Equation (2), where the intensity of oil-polluted seawater ($I(\lambda_{Em\ of\ oil\text{-}polluted\ seawater})$) is divided by the intensity of oil-free seawater ($I(\lambda_{Em\ of\ oil\text{-}free\ seawater})$) at 340/355 for λ_{Ex} = 225 nm.

$$FI_{o/w} = \left[\frac{I(\lambda_{Emission\ of\ seawater\ polluted\ by\ oil})}{I(\lambda_{Emission\ of\ natural(oil-free)\ seawater})}\right]_{\lambda_{Excitation}} \quad (1)$$

$$FI_{o/w} = \left[\frac{I(\lambda_{Em=340})}{I(\lambda_{Em=355})}\right]_{\lambda_{Ex=225}} \quad (2)$$

The FI was established with specific criteria to determine the presence of oil pollution in seawater. According to these criteria, FI values above 1 indicate the presence of oil in the water, whereas FI values below 1 indicate that the seawater is free from oil contamination. The FI was calculated for oil-polluted seawater for specific months within the $r_{o/w}$ range of

0.5–500 × 10^{-6}. Table 6 shows the obtained $FI_{o/w}$ values for polluted seawater from April to March 2019–2020, with the Baltic Sea divided into productive and unproductive seasons throughout the year. The $FI_{o/w}$ values for oil-polluted seawater range from 1.72 to 1.67 for the highest $r_{o/w}$ (500 × 10^{-6}), while for the lowest $r_{o/w}$ (0.5 × 10^{-6}), the $FI_{o/w}$ variations range from 1.12–1.44. It can be concluded that $FI_{o/w}$ values for oil-polluted seawater are independent of biological activity, which fluctuates during productive and unproductive seasons in the Baltic Sea within the considered $r_{o/w}$ range of 0.5–500 × 10^{-6}. Additionally, $FI_{o/w}$ values are not dependent on specific months. Table 7 shows that the $FI_{o/w}$ values for oil-free seawater vary from 0.86 in April, when biological activity is high, to 0.80 in February, when biological activity is low. Higher FI values can be observed during the productive season, ranging from 0.86 to 0.81, with an average value of 0.85, while lower FI values are observed during the unproductive season, ranging from 0.84–0.8, with an average value of 0.81. Finally, the obtained results of $FI_{o/w}$ for oil-polluted seawater in the range of $r_{o/w}$ from 0.5 × 10^{-6} to 500 × 10^{-6} do not depend on the biological activity in the Baltic Sea or on the month. It should be highlighted that $FI_{o/w}$ values for oil-polluted seawater for $r_{o/w}$ in the range 50–200 × 10^{-9} analyzed in the previous papers [51,52] depend on the biological activity. Based on the analysis of the results, it can be concluded that the proposed method for detecting oil in water, based on the fluorimetric index (FI), functions accurately within the specified range of oil-to-water ratios ($r_{o/w}$). When oil was present in the water during individual months throughout the year, the FI consistently indicated its presence by attaining values higher than 1. Conversely, for unpolluted seawater, the FI consistently yielded values below 1. It is worth noting that FI values are influenced by the $r_{o/w}$ ratio, but throughout the entire year, for a given $r_{o/w}$ ratio, the FI values exhibited negligible fluctuations.

Table 6. $FI_{o/w}$ values calculated for contaminated seawater with an oils mixture for particular $r_{o/w}$ from April to December in 2019 and from January to March in 2020.

	$FI_{o/w}$ [-]			
$r_{o/w}$	0.5 × 10^{-6}	50 × 10^{-6}	100 × 10^{-6}	500 × 10^{-6}
April	1.44	1.43	1.69	1.72
May	1.26	1.40	1.65	1.68
June	1.18	1.36	1.68	1.70
July	1.42	1.53	1.66	1.72
August	1.34	1.39	1.64	1.67
September	1.37	1.38	1.67	1.73
October	1.20	1.34	1.67	1.68
November	1.34	1.33	1.69	1.68
December	1.24	1.41	1.65	1.71
January	1.28	1.40	1.70	1.71
February	1.12	1.41	1.69	1.69
March	1.35	1.44	1.66	1.68

Table 7. $FI_{o/w}$ values calculated for natural seawater sampled for particular months from April to December 2019 and from January to March 2020.

	$FI_{o/w}$ [-]
	Natural Seawater
April	0.86
May	0.86
June	0.87
July	0.87
August	0.86
September	0.81
October	0.85
November	0.80
December	0.82
January	0.80
February	0.83
March	0.84

4. Conclusions

The objective of the study was to indicate the correct functioning of the fluorometric index (FI) as a tool for detecting oil regardless of changes in the content of natural seawater components throughout the entire year. In the fluorescence spectra of all oil-free and oil-contacted water samples, excitation-emission (EEM) peaks were observed that partially overlap. However, the spectral fluorescence index (FI) used was found to be a parameter indicating the presence of oil in various seasons.

The obtained data provide the basis for predicting the efficacy of the fluorometric index. Overall results of FI indicate that particular months achieved similar values in relation to a given $r_{o/w}$ and do not show seasonal dependence in the considered oil-to-water ratio range. Moreover, the position of determined excitation-emission peaks for a particular month and different oil-to-water ratios do not change when the natural seawater fluorescence is subtracted from the EEM spectrum. Summing up, the fluorescence of natural seawater constituents does not disturb or obscure oil fluorescence in the considered oil-to-water ratio range. The monitoring of biological components of the sea and their dynamics is necessary, as well as the monitoring of oil pollution using available methods. Models for tracking changes in marine components require additions to oily substances and constant updating. The obtained optical parameters of the oil dissolved in water will complement the environmental models to track the phytoplankton or colored organic matter. The data also can be used as input data for operational models for tracking marine components or detecting petroleum substances in the sea. Moreover, the data of FI can be used in the construction of underwater tools to signal the presence of oil.

Author Contributions: Conceptualization, E.B. and Z.O.; methodology, E.B.; formal analysis, E.B.; investigation, E.B. and Z.O.; data curation, E.B. and Z.O.; writing—original draft preparation, E.B.; writing—review and editing, Z.O.; visualization, E.B. and Z.O. All authors have read and agreed to the published version of the manuscript.

Funding: This research received no external funding.

Institutional Review Board Statement: Not applicable.

Informed Consent Statement: Not applicable.

Data Availability Statement: Not applicable.

Acknowledgments: The work contained in this paper was supported by a Gdynia Maritime University grants, No. WM/2023/PI/01, WM/2023/PZ/04, WM/2023/PZ/06. The authors would like to thank H. Toczek, R. Maksyś and W. Targowski for their assistance with the measurements.

Conflicts of Interest: The authors declare no conflict of interest.

References

1. Fingas, M. *Oil Spill Science and Technology*; Gulf Professional Publishing: Houston: Houston, TX, USA; Elsevier: Amsterdam, The Netherlands, 2011.
2. Fingas, M. *The Basics of Oil Spill Cleanup*, 3rd ed.; CRC Press: Boca Raton, FL, USA, 2012.
3. Fingas, M.; Brown, C.E. Oil spill remote sensing. In *Earth System Monitoring: Selected Entries from the Encyclopedia of Sustainability Science and Technology*; Orcutt, J., Ed.; Springer: Berlin/Heidelberg, Germany, 2013; pp. 337–388. [CrossRef]
4. Fingas, M. Marine Oil Spills 2018. *J. Mar. Sci. Eng.* **2019**, *7*, 82. [CrossRef]
5. White, H.K.; Hsing, P.-Y.; Cho, W.; Shank, T.M.; Cordes, E.E.; Quattrini, A.M.; Nelson, R.K.; Camilli, R.; Demopoulos, A.W.J.; German, C.R.; et al. Impact of the Deepwater Horizon oil spill on a deep-water coral community in the Gulf of Mexico. *Proc. Natl. Acad. Sci. USA* **2012**, *109*, 20303–20308. [CrossRef] [PubMed]
6. Hu, C.; Feng, L.; Holmes, J.; Swayze, G.A.; Leifer, I.; Melton, C.; Garcia, O.; Macdonald, I.; Hess, M.; Muller-Karger, F.; et al. Remote sensing estimation of surface oil volume during the 2010 Deepwater Horizon oil blowout in the Gulf of Mexico: Scaling up AVIRIS observations with MODIS measurements. *J. Appl. Rem. Sens.* **2018**, *12*, 026008. [CrossRef]
7. Kujawinski, E.B.; Reddy, C.M.; Rodgers, R.P.; Thrash, J.C.; Valentine, D.L.; White, H.K. The first decade of scientific insights from the Deepwater Horizon oil release. *Nat. Rev. Earth Environ.* **2020**, *1*, 237–250. [CrossRef]
8. Transport Volume of Crude Oil in Seaborne Trade Worldwide from 2010 to 2021. Available online: https://www.statista.com/statistics/264013/transport-volume-of-crude-oil-in-seaborne-trade/ (accessed on 27 April 2023).

9. Baltic Lines. Shipping in the Baltic Sea. Past, Present and Future Developments Relevant for Maritime Spatial Planning. Available online: https://vasab.org/wp-content/uploads/2018/06/Baltic-LINes-Shipping_Report-20122016.pdf (accessed on 23 May 2023).
10. IMO. The International Convention for the Prevention of Pollution from Ships (MARPOL), 1973, as Modified by the Protocol of 1978. Available online: http://www.imo.org/en/About/conventions/listofconventions/pages/international-convention-for-the-prevention-of-pollution-from-ships-(marpol).aspx (accessed on 27 April 2023).
11. Gennaro, M. Oil Pollution Liability and Control under International Maritime Law: Market Incentives as an Alternative to Government Regulation. *Vanderbilt J. Transnatl. Law* **2004**, *37*, 265–298.
12. Illegal Discharges of Oil in the Baltic Sea Baltic Sea Environment Fact Sheet 2016, Published 11 July 2016. Available online: https://helcom.fi/wp-content/uploads/2020/08/Illegal-Discharges-of-Oil-in-the-Baltic-Sea.pdf (accessed on 27 April 2023).
13. Al-Ruzouq, R.; Gibril, M.B.A.; Shanableh, A.; Kais, A.; Hamed, O.; Al-Mansoori, S.; Khalil, M.A. Sensors, Features, and Machine Learning for Oil Spill Detection and Monitoring: A Review. *Remote Sens.* **2020**, *12*, 3338. [CrossRef]
14. Pärt, S.; Kankaanpää, H.; Björkqvist, J.-V.; Uiboupin, R. Oil Spill Detection Using Fluorometric Sensors: Laboratory Validation and Implementation to a FerryBox and a Moored SmartBuoy. *Front. Mar. Sci.* **2021**, *8*, 778136. [CrossRef]
15. Hu, C.; Lu, Y.; Sun, S.; Liu, Y. Optical Remote Sensing of Oil Spills in the Ocean: What Is Really Possible? *J. Remote Sens.* **2021**, *2021*, 9141902. [CrossRef]
16. Hou, Y.; Li, Y.; Li, G.; Tong, X.; Wang, Y. Oil-spill detection sensor using ultraviolet-induced fluorescence for routine surveillance in coastal environments. *Appl. Phys. B* **2022**, *128*, 41. [CrossRef]
17. Response to Spills. Available online: https://helcom.fi/action-areas/response-to-spills/ (accessed on 27 April 2023).
18. Alpers, W.; Holt, B.; Zeng, K. Remote sensing of environment oil spill detection by imaging radars: Challenges and pitfalls. *Remote Sens. Environ.* **2017**, *201*, 133–147. [CrossRef]
19. Tysiąc, P.; Strelets, T.; Tuszyńska, W. The Application of Satellite Image Analysis in Oil Spill Detection. *Appl. Sci.* **2022**, *12*, 4016. [CrossRef]
20. Sun, S.; Hu, C. The challenges of interpreting oil-water spatial and spectral contrasts for the estimation of oil thickness: Examples from satellite and airborne measurements of the Deepwater Horizon oil spill. *IEEE Trans. Geosci. Remote Sens.* **2019**, *57*, 2643–2658. [CrossRef]
21. Conceição, M.R.A.; de Mendonça, L.F.F.; Lentini, C.A.D.; da Cunha Lima, A.T.; Lopes, J.M.; de Vasconcelos, R.N.; Gouveia, M.B.; Porsani, M.J. SAR Oil Spill Detection System through Random Forest Classifiers. *Remote Sens.* **2021**, *13*, 2044. [CrossRef]
22. Li, X.; Li, C.; Yang, Z.; Pichel, W. SAR imaging of ocean surface oil seep trajectories induced by near-inertial oscillation. *Remote Sens. Environ.* **2013**, *130*, 182–187. [CrossRef]
23. Chen, G.; Li, Y.; Sun, G.; Zhang, Y. Application of deep networks to oil spill detection using polarimetric synthetic aperture radar images. *Appl. Sci.* **2017**, *7*, 968. [CrossRef]
24. EMSA (European Maritime Safety Agency) Outlook 2023. Available online: https://www.emsa.europa.eu/ (accessed on 27 April 2023).
25. CleanSeaNet Service Detections and Feedback Data 2021, EMSA; in CleanSeaNet—Detections and Feedback Data (2015–2021). Available online: https://www.emsa.europa.eu/we-do/surveillance/earthobservationservices/item/4645-cleanseanet-detections-and-feedback-data.html (accessed on 27 April 2023).
26. Chekalyuk, A.; Hafez, M. Next generation Advanced Laser Fluorometry (ALF) for characterization of natural aquatic environments: New instruments. *Opt Express* **2013**, *21*, 14181. [CrossRef]
27. Xie, M.; Jia, Y.; Li, Y.; Cai, X.; Cao, K. Experimental Analysis on the Optimal Excitation Wavelength for Fine-Grained Identification of Refined Oil Pollutants on WaterSurface Based on Laser-Induced Fluorescence. *J. Fluoresc.* **2022**, *32*, 257–265. [CrossRef]
28. Li, Y.; Jia, Y.; Cai, X.; Xie, M.; Zhang, Z. Oil pollutant identification based on excitation-emission matrix of UV-induced fluorescence and deep convolutional neural network. *Environ. Sci. Pollut. Res.* **2022**, *29*, 68152–68160. [CrossRef]
29. Fingas, M.; Brown, C. A Review of oil spill remote sensing. *Sensors* **2017**, *18*, 91. [CrossRef]
30. Wang, Z.; Stout, S. *Oil Spill Environmental Forensics: Fingerprinting and Source Identification*, 2nd ed.; Academic Press: London, UK, 2016.
31. Chepyzhenko, A.A.; Lomakin, P.D.; Chepyzhenko, A.I. Methods and device for dissolved oil in water environment in-situ monitoring. In *Atmospheric and Ocean Optics*; SPIE: St. Bellingham, WA, USA, 2020.
32. Geng, T.; Wang, Y.; Yin, X.-L.; Chen, W. A Comprehensive Review on the Excitation-Emission Matrix Fluorescence Spectroscopic Characterization of Petroleum-Containing Substances: Principles, Methods, and Applications. *Crit. Rev. Anal. Chem.* **2023**, *8*, 1–23. [CrossRef]
33. Conmy, R.N.; Coble, P.G.; Farr, J.; Wood, A.M.; Lee, K.; Pegau, W.S.; Walsh, I.D.; Koch, C.R.; Abercrombie, M.I.; Miles, M.S.; et al. Submersible Optical Sensors Exposed to Chemically Dispersed Crude Oil: Wave Tank Simulations for Improved Oil Spill Monitoring. *Environ. Sci. Technol.* **2014**, *48*, 1803–1810. [CrossRef] [PubMed]
34. Ferdinand, O.D.; Friedrichs, A.; Miranda, M.L.; Voß, D.; Zielinski, O. Next-generation fluorescence sensor with multiple excitation and emission wavelengths—NeXOS MatrixFlu-UV. In Proceedings of the OCEANS-2017, Abredeen, UK, 19–22 June 2017; IEEE: Piscataway, NJ, USA, 2017. [CrossRef]

35. Elsherif, M.; Salih, A.E.; Muñoz Monserrat, G.; Alam, F.; AlQattan, B.; Antonysamy, D.S.; Zaki, M.F.; Yetisen, A.K.; Park, S.; Wilkinson, T.D.; et al. Optical Fiber Sensors: Working Principle, Applications, and Limitations. *Adv. Photonics Res.* **2022**, *3*, 2100371. [CrossRef]
36. Woźniak, S.B.; Meler, J.; Lednicka, B.; Zdun, A.; Stoń-Egiert, J. Inherent optical properties of suspended particulate matter in the southern Baltic Sea. *Oceanologia* **2011**, *53*, 691–729.
37. Soja-Woźniak, M.; Craig, S.E.; Wojtasiewicz, B.; Kratzer, S.; Darecki, M.; Jones, C.T. A Novel Statistical Approach for Ocean Colour Estimation of Inherent Optical Properties and Cyanobacteria Abundance in Optically Complex Waters. *Remote Sens.* **2017**, *9*, 343. [CrossRef]
38. Meler, J.; Kowalczuk, P.; Ostrowska, M.; Ficek, D.; Zabłocka, M.; Zdun, A. Parameterization of the light absorption properties of chromophoric dissolved organic matter in the Baltic Sea and Pomeranian lakes. *Ocean. Sci.* **2016**, *12*, 1013–1032. [CrossRef]
39. Ostrowska, M. Model dependences of the deactivation of phytoplankton pigment excitation energy on environmental conditions in the sea. *Oceanology* **2012**, *54*, 545–564. [CrossRef]
40. McKee, D.; Röttgers, R.; Neukermans, G.; Calzado, V.S.; Trees, C.; Ampolo-Rella, M.; Neil, C.; Cunningham, A. Impact of measurement uncertainties on determination of chlorophyll-specific absorption coefficient for marine phytoplankton. *J. Geophys. Res. Oceans* **2014**, *119*, 9013–9025. [CrossRef]
41. Coble, P.G. Characterization of marine and terrestrial DOM in seawater using excitation-emission matrix spectroscope. *Mar. Chem.* **1996**, *51*, 325–346. [CrossRef]
42. Drozdowska, V.; Wrobel, I.; Markuszewski, P.; Makuch, P.; Raczkowska, A.; Kowalczuk, P. Study on organic matter fractions in the surface microlayer in the Baltic Sea by spectrophotometric and spectrofluorometric methods. *Ocean Sci.* **2017**, *13*, 633–647. [CrossRef]
43. Drozdowska, V.; Kowalczuk, P.; Konik, M.; Dzierzbicka-Glowacka, L. Study on Different Fractions of Organic Molecules in the Baltic Sea Surface Microlayer by Spectrophoto- and Spectrofluorimetric Methods. *Front. Mar. Sci.* **2018**, *5*, 456. [CrossRef]
44. Miranda, M.L.; Mustaffa, N.I.H.; Robinson, T.-B.; Stolle, C.; Ribas-Ribas, M.; Wurl, O.; Zielinski, O. Influence of solar radiation on biogeochemical parameters and fluorescent dissolved organic matter (FDOM) in the sea surface microlayer of the southern coastal North Sea. *Elem. Sci. Anth.* **2018**, *6*, 15. [CrossRef]
45. Zielinski, O.; Rüssmeier, N.; Ferdinand, O.D.; Miranda, M.L.; Wollschläger, J. Assessing Fluorescent Organic Matter in Natural Waters: Towards In Situ Excitation–Emission Matrix Spectroscopy. *Appl. Sci.* **2018**, *8*, 2685. [CrossRef]
46. Kowalczuk, P.; Cooper, W.J.; Durako, M.J.; Kahn, A.E.; Gonsior, M.; Young, H. Characterization of dissolved organic matter fluorescence in the South Atlantic bight with use of PARAFAC model: Relationships between fluorescence and its components, absorption coefficients and organic carbon concentrations. *Mar. Chem.* **2010**, *118*, 22–36. [CrossRef]
47. Baszanowska, E.; Otremba, Z. Modification of optical properties of seawater exposed to oil contaminants based on excitation-emission spectra. *J. Eur. Opt. Soc. Rapid Publ.* **2015**, *10*, 10047. [CrossRef]
48. Ecohydrodynamic Forecast for the Baltic Sea. Available online: http://model.ocean.univ.gda.pl/php/frame.php?area=ZatokaGdanska (accessed on 27 April 2023).
49. Coble, P. Colored dissolved organic matter in seawater. In *Subsea Optics and Imaging*; Elsevier BV: London, UK, 2013; pp. 98–118.
50. Drozdowska, V.; Freda, W.; Baszanowska, E.; Rudź, K.; Darecki, M.; Heldt, J.; Toczek, H. Spectral properties of natural and oil-polluted Baltic seawater—Results of measurements and modelling. *Eur. Phys. J. Spec. Top.* **2013**, *222*, 2157–2170. [CrossRef]
51. Baszanowska, E.; Otremba, Z. Fluorometric Detection of Oil Traces in a Sea Water Column. *Sensors* **2022**, *22*, 2039. [CrossRef] [PubMed]
52. Baszanowska, E.; Otremba, Z. Detection of Oil in Seawater Based on the Fluorometric Index during the Winter Season in the Baltic Sea—The Case of the Gulf of Gdansk. *Sensors* **2022**, *22*, 6014. [CrossRef]
53. Baszanowska, E.; Otremba, Z. Detecting the Presence of Different Types of Oil in Seawater Using a Fluorometric Index. *Sensors* **2019**, *19*, 3774. [CrossRef]
54. Kowalczuk, P.; Stedmon, C.A.; Markager, M. Modeling absorption by CDOM in the Baltic Sea from the season, salinity and chlorophyll. *Mar. Chem.* **2006**, *101*, 1–11. [CrossRef]

Disclaimer/Publisher's Note: The statements, opinions and data contained in all publications are solely those of the individual author(s) and contributor(s) and not of MDPI and/or the editor(s). MDPI and/or the editor(s) disclaim responsibility for any injury to people or property resulting from any ideas, methods, instructions or products referred to in the content.